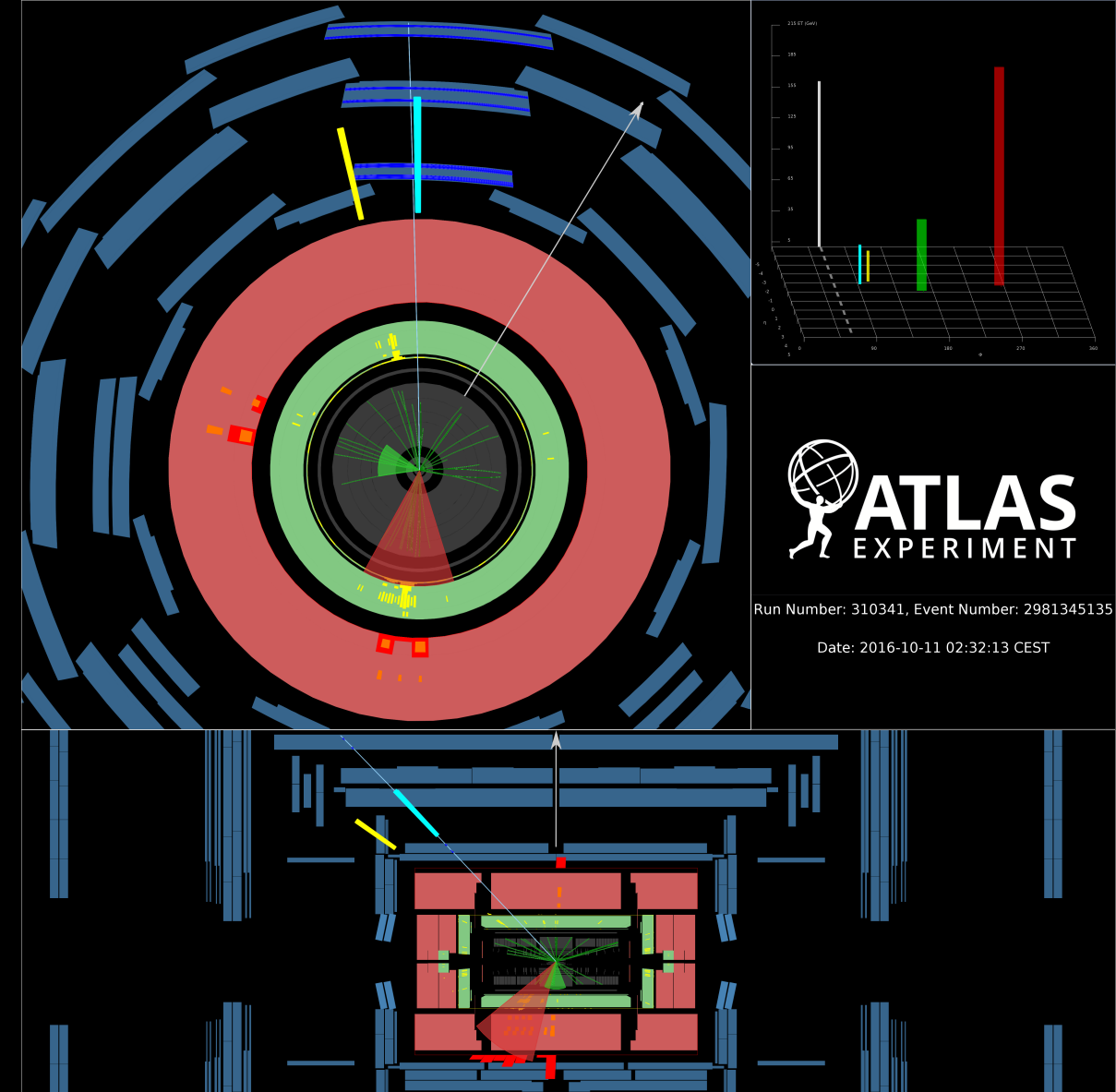


# Measurements and Interpretations of STXS and Differential and Fiducial Cross Sections in Higgs Boson Decays to two $W$ Bosons with the ATLAS Detector

Robin Hayes on behalf of the ATLAS Collaboration

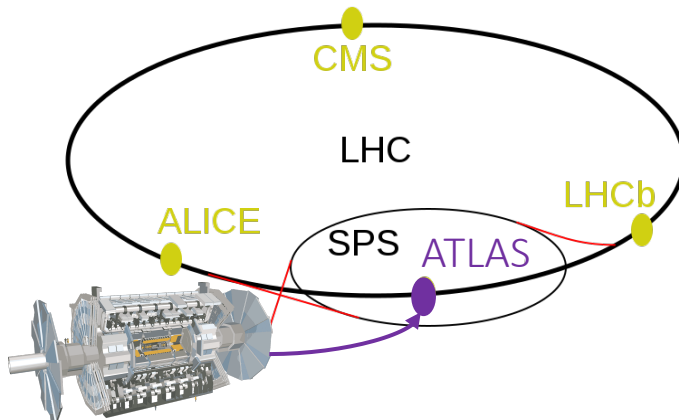
Higgs 2021  
Oct. 18-22 2021



# Probing Higgs Production with $H \rightarrow WW^*$

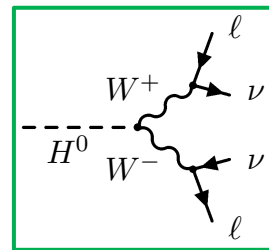
## Beyond Signal Strengths

- Standard in Higgs boson measurements: production cross-section(s) and signal strength.
- More recently: differential, fiducial and Simplified Template Cross Sections (STXS) measurements.
  - Big advantage: interpretable (more easily), eg. in the Effective Field Theory (EFT) framework.

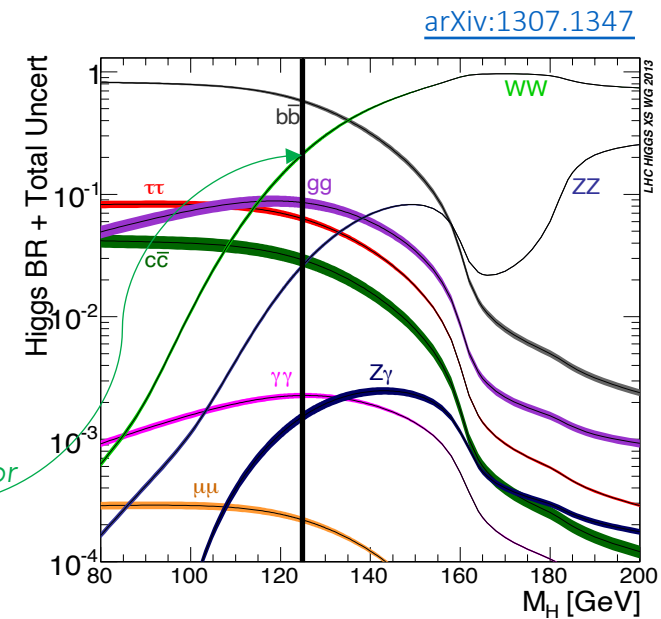


## Why $H \rightarrow WW^*$ ?

- Second largest Higgs branching ratio.
- Leptonic decay useful for distinguishing signal.



Branching ratio for  
 $H \rightarrow WW^*$  at  
 $m_H = 125$  GeV.



## Analyses Featured Today

- Come from data collected by the ATLAS detector at  $\sqrt{s} = 13$  TeV.
- Measurement of ggF and VBF STXS cross-sections ( $139\text{ fb}^{-1}$ ): [ATLAS-CONF-2021-014](#)
- EFT interpretation of  $WW$  and  $H \rightarrow WW^*$  results ( $36\text{ fb}^{-1}$ ): [ATL-PHYS-PUB-2021-010](#)

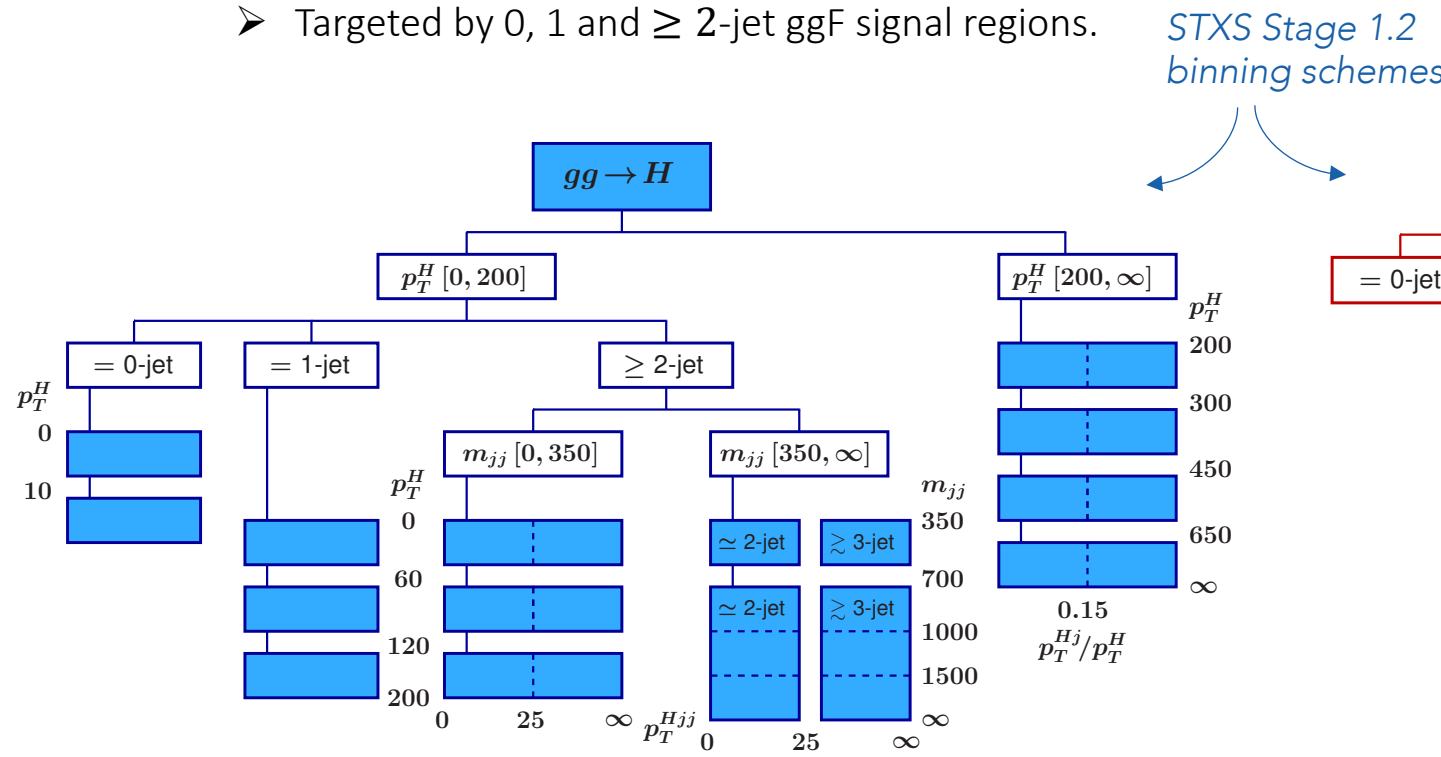
# ggF & VBF $H \rightarrow WW^*$ STXS

Analysis Scope: [ATLAS-CONF-2021-014](#)

- ggF and VBF production of Higgs bosons in the  $H \rightarrow WW^* \rightarrow e\nu\mu\nu$  decay channel.
- Measure 11 cross-sections in phase spaces defined by the STXS framework, using **full Run 2 data**.

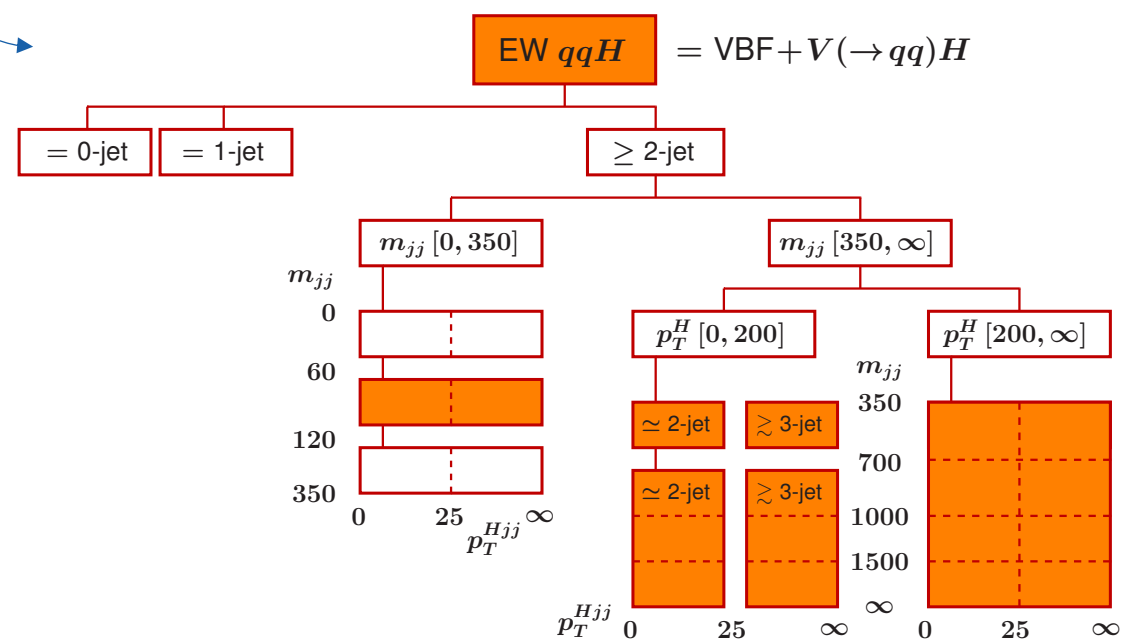
## ggH production:

- Measure 6 cross-sections
- Targeted by 0, 1 and  $\geq 2$ -jet ggF signal regions.



## EW qqH production:

- Measure 5 cross-sections
- Targeted by  $\geq 2$ -jet VBF signal regions.



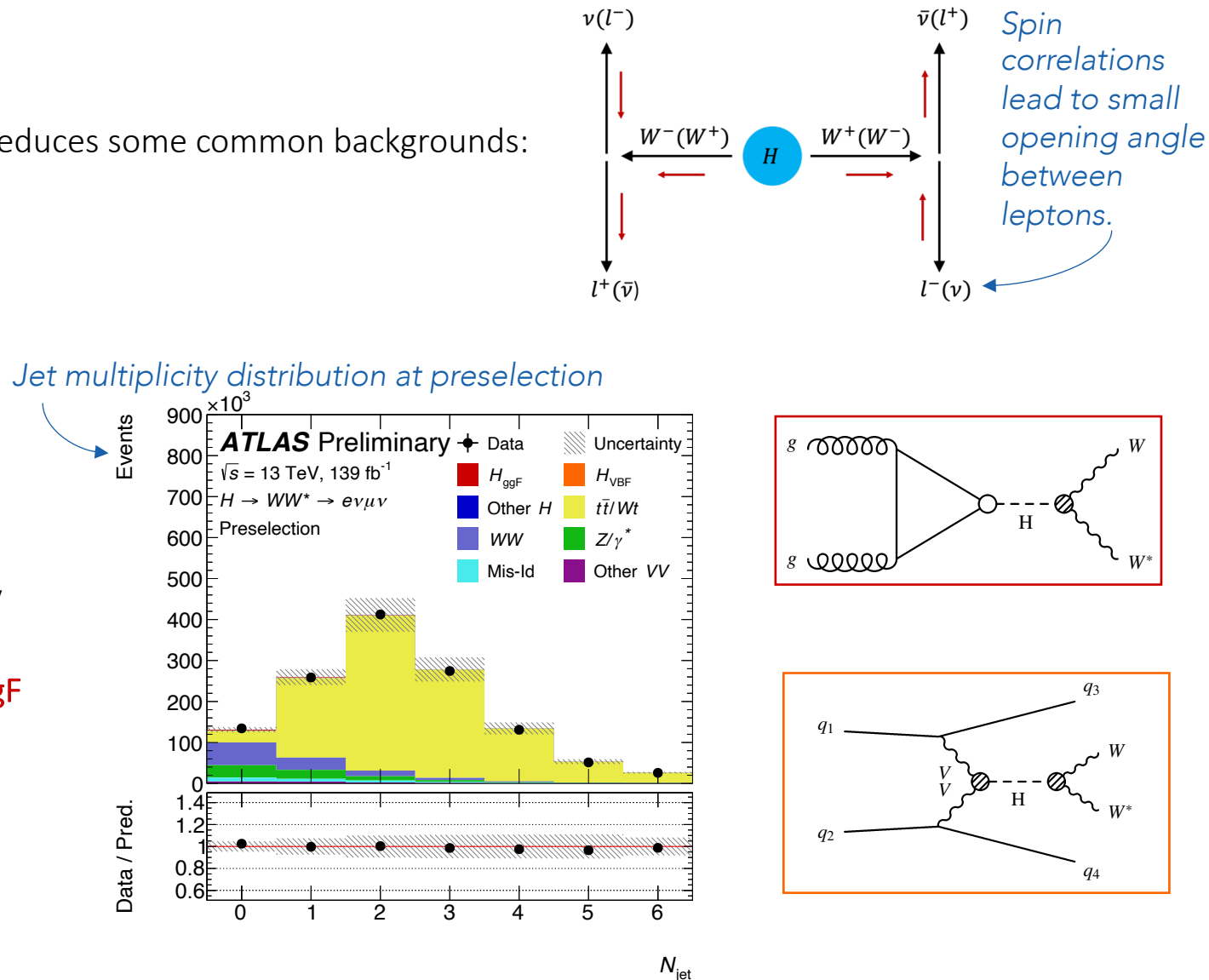
# Preselection and Analysis Channels

## Common Preselection:

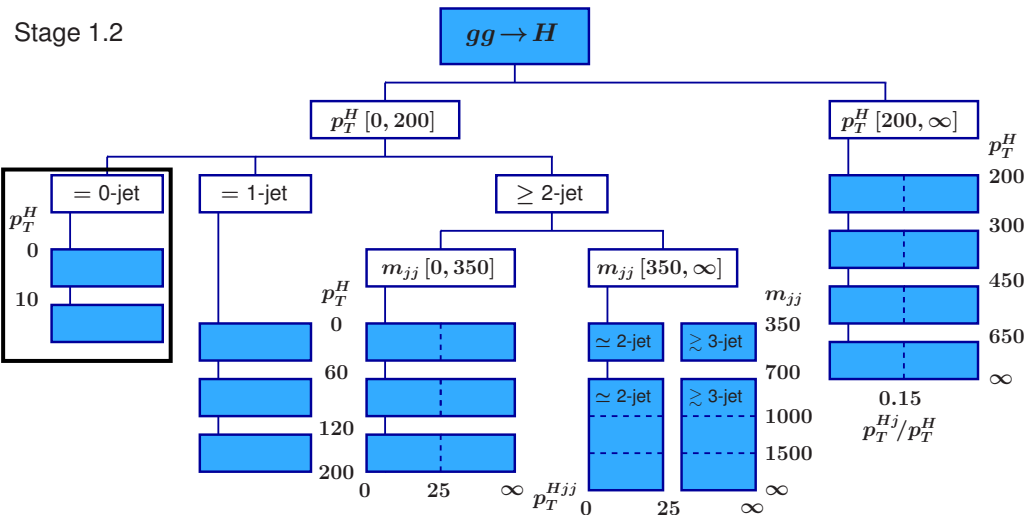
- Targets features of  $H \rightarrow WW^* \rightarrow e\nu\mu\nu$  decay and reduces some common backgrounds:
  - ✓ Single-lepton and dilepton triggers used
  - ✓ 2 different-flavour, opposite-charge leptons
  - ✓  $p_T^{\text{lead}} > 22 \text{ GeV}$ ,  $p_T^{\text{sublead}} > 15 \text{ GeV}$
  - ✓  $m_{ll} > 10 \text{ GeV}$
  - ✓  $p_T^{\text{miss}} > 20 \text{ GeV}$  (ggF channels only)

## Defining Analysis Channels:

- Channels split by number of jets with  $p_T > 30 \text{ GeV}$  after preselection:
  - $N_{\text{jets}} = 0$  and  $N_{\text{jets}} = 1$  channels to target **ggF**
  - $N_{\text{jets}} \geq 2$  channels to target **ggF** and **VBF**
- Motivated by differing background compositions in each region.
- Remaining cuts are targeted to each analysis category.



# ggF 0-jet Signal Region



## Background rejection

- ✓  $N_{b\text{-jet}}^{p_T > 20 \text{ GeV}} = 0$
- ✓  $\Delta\phi_{ll, E_T^{\text{miss}}} > \pi/2$
- ✓  $p_T^{ll} > 30 \text{ GeV}$

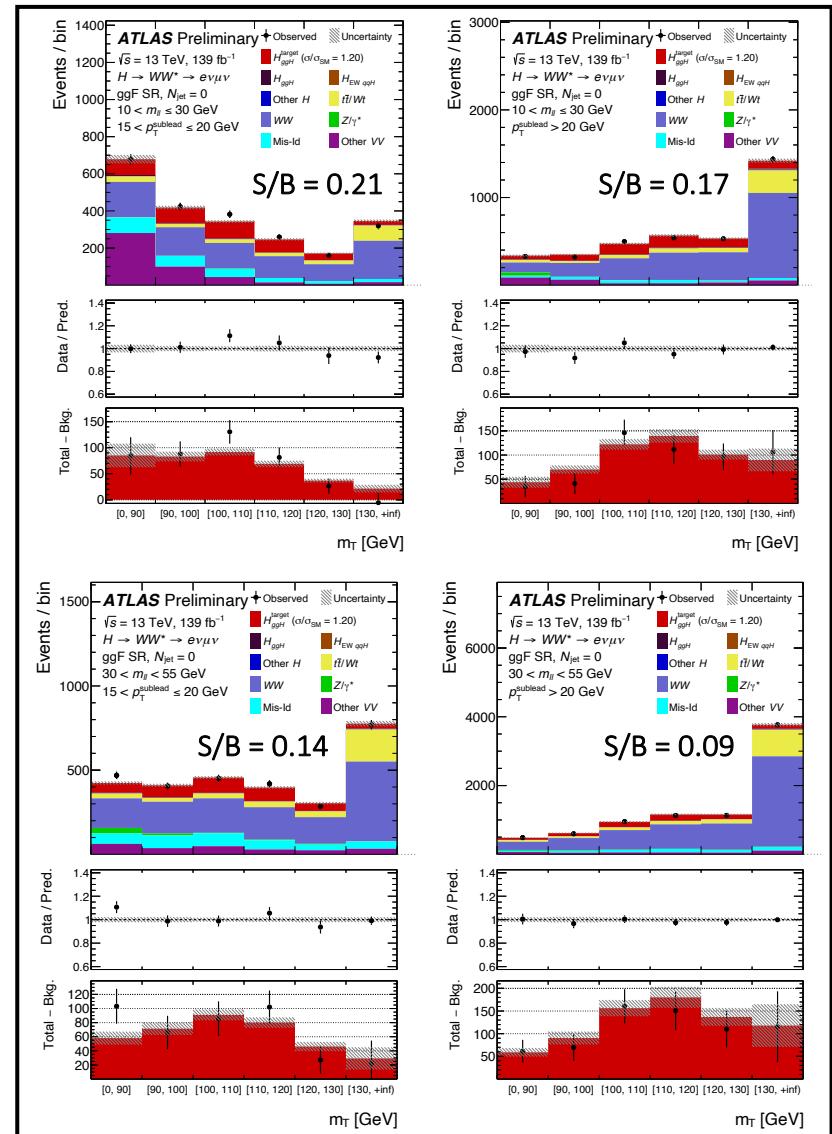
## $H \rightarrow WW^* \rightarrow e\nu\mu\nu$ topology

- ✓  $m_{ll} < 55 \text{ GeV}$
- ✓  $\Delta\phi_{ll} < 1.8$

Control regions for top,  $qqWW$ ,  $Z/\gamma^*$  backgrounds.

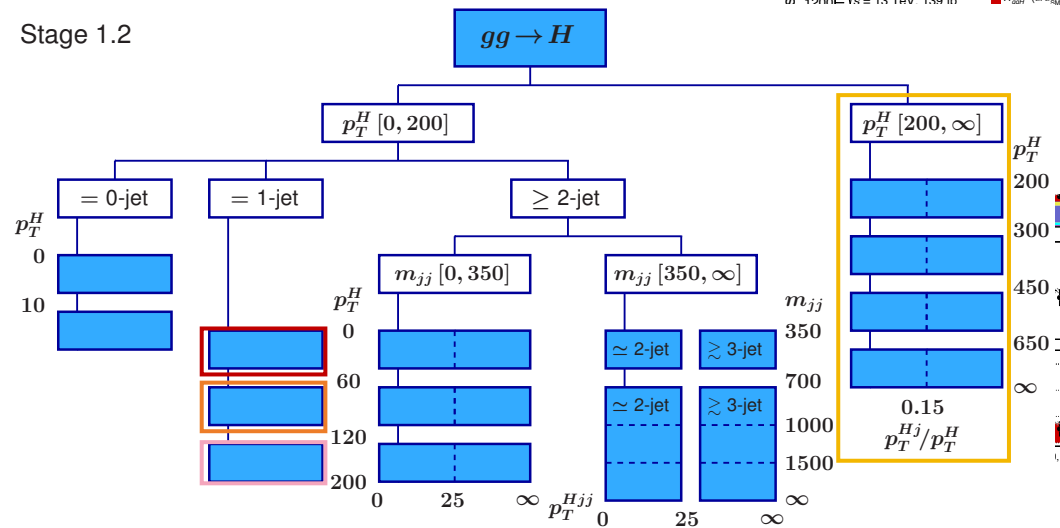
## Final discriminant:

$$m_T = \sqrt{(E_T^{\text{miss}} + E_T^{ll})^2 - |\vec{E_T^{\text{miss}}} + \vec{p_T^{ll}}|^2}$$



# ggF 1-jet Signal Region

Stage 1.2



## Background rejection

- ✓  $N_{b\text{-jet}}^{p_T > 20 \text{ GeV}} = 0$
- ✓  $m_{\tau\tau} < m_Z - 25 \text{ GeV}$
- ✓  $\max(m_T^l) > 50 \text{ GeV}$

Re-constructed using  
the collinear  
approximation  
[\[arXiv:hep-ph/9911385\]](https://arxiv.org/abs/hep-ph/9911385)

## $H \rightarrow WW^* \rightarrow e\nu\mu\nu$ topology

- ✓  $m_{ll} < 55 \text{ GeV}$
- ✓  $\Delta\phi_{ll} < 1.8$

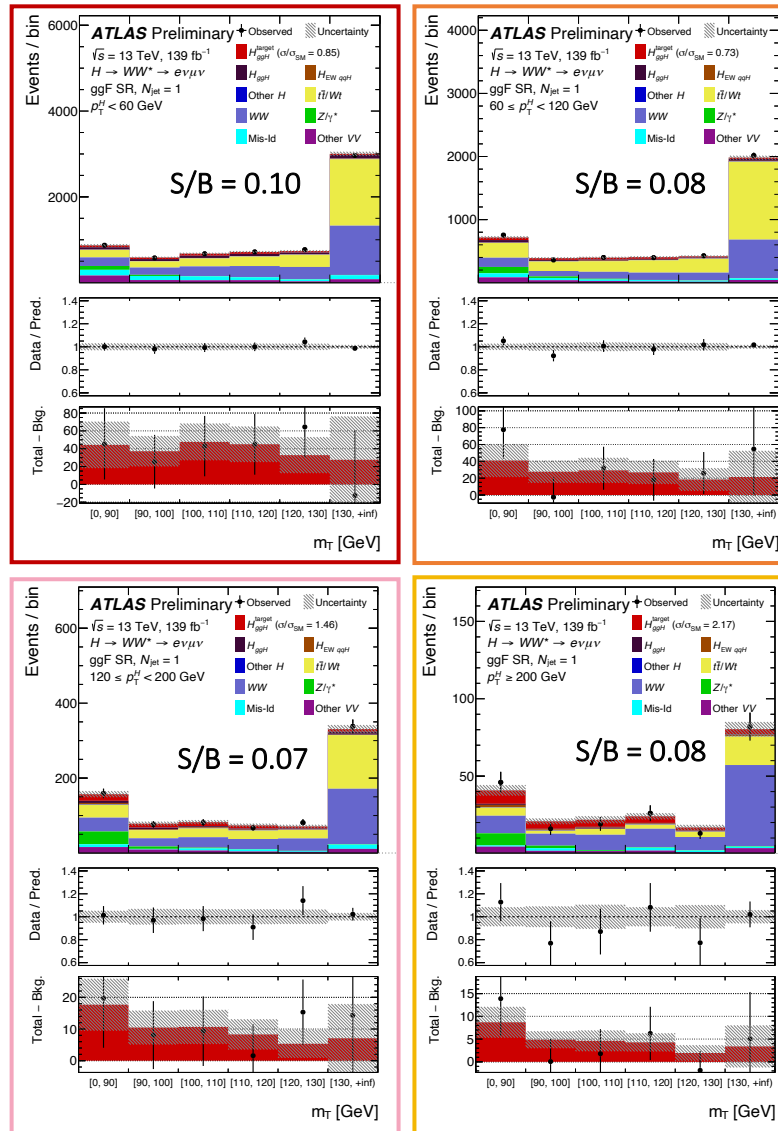
Control regions for top,  $qqWW$ ,  $Z/\gamma^*$  backgrounds.

## Final discriminant:

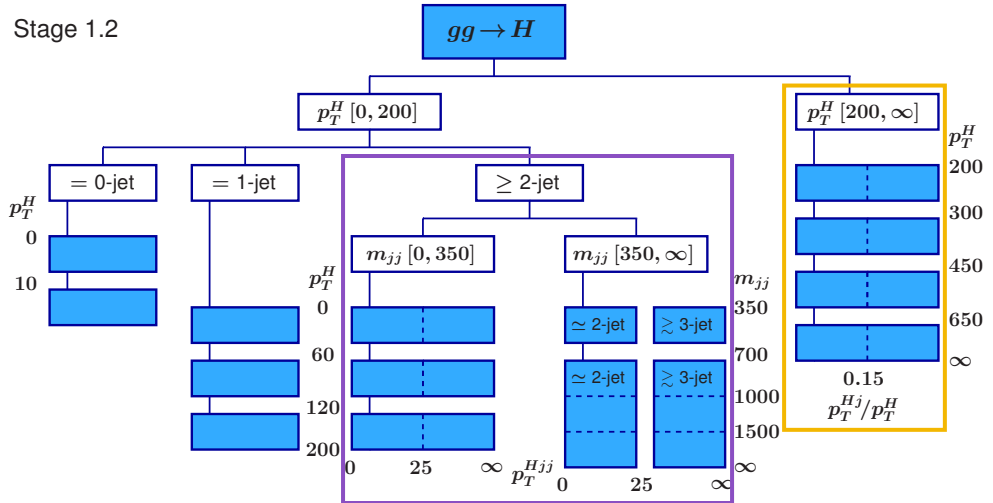
$$m_T = \sqrt{(E_T^{\text{miss}} + E_T^l)^2 - |\vec{E}_T^{\text{miss}} + \vec{p}_T^l|^2}$$

Split by:

$$p_T^H = |\vec{p}_T^l + \vec{E}_T^{\text{miss}}|$$



# ggF $\geq 2$ -jet Signal Region



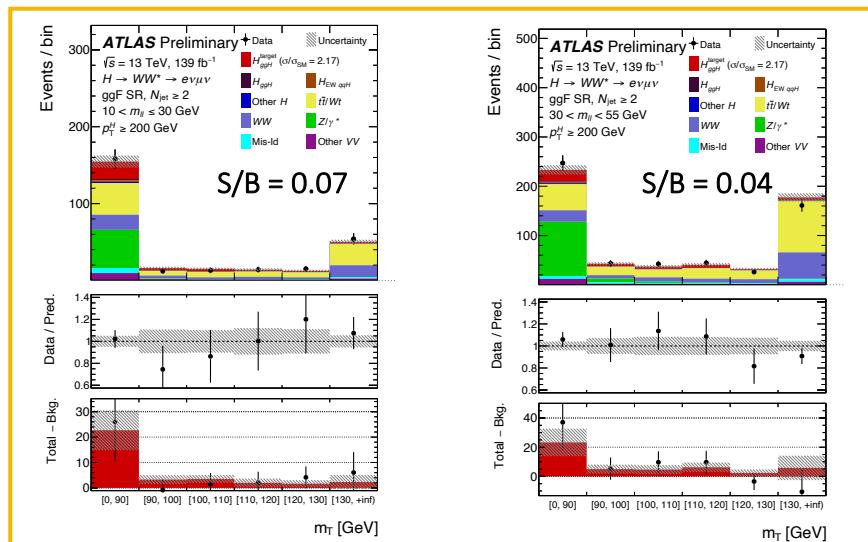
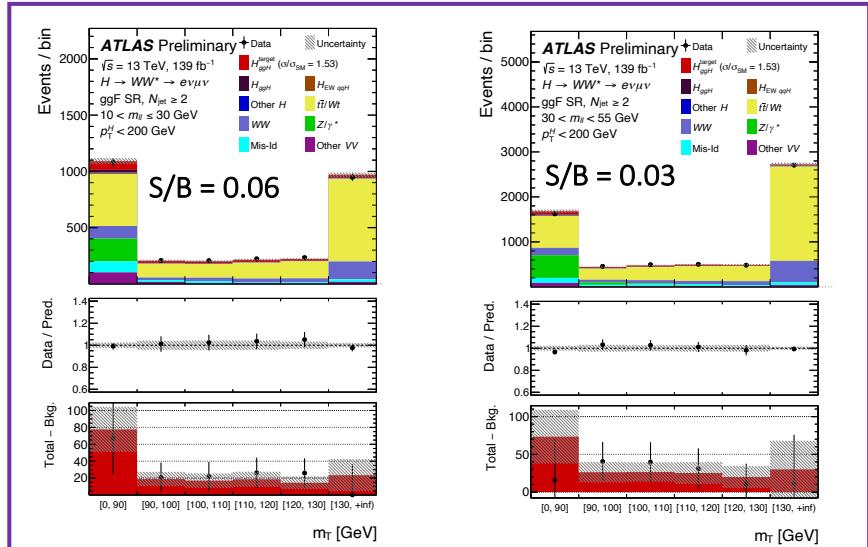
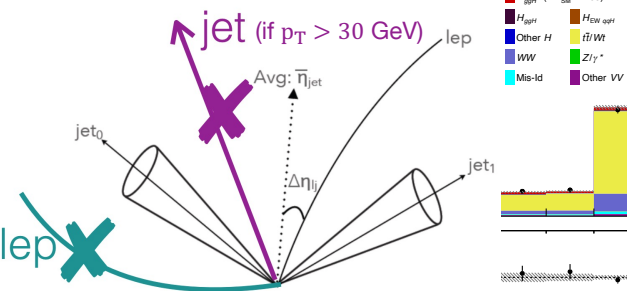
## Background rejection

- ✓  $N_{b\text{-jet}}^{p_T > 20 \text{ GeV}} = 0$
- ✓  $m_{\tau\tau} < m_Z - 25 \text{ GeV}$

## $H \rightarrow WW^* \rightarrow e\nu\mu\nu$ topology

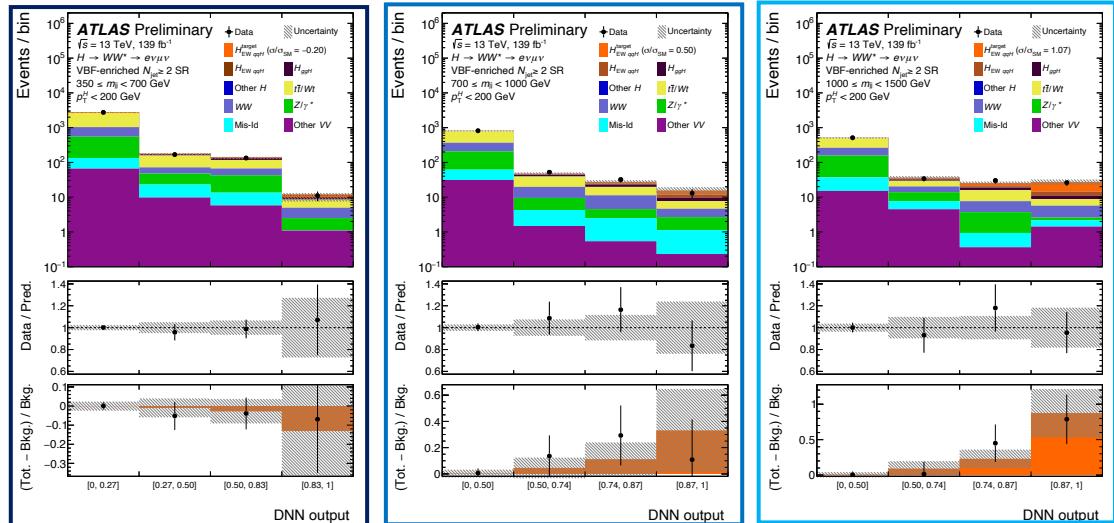
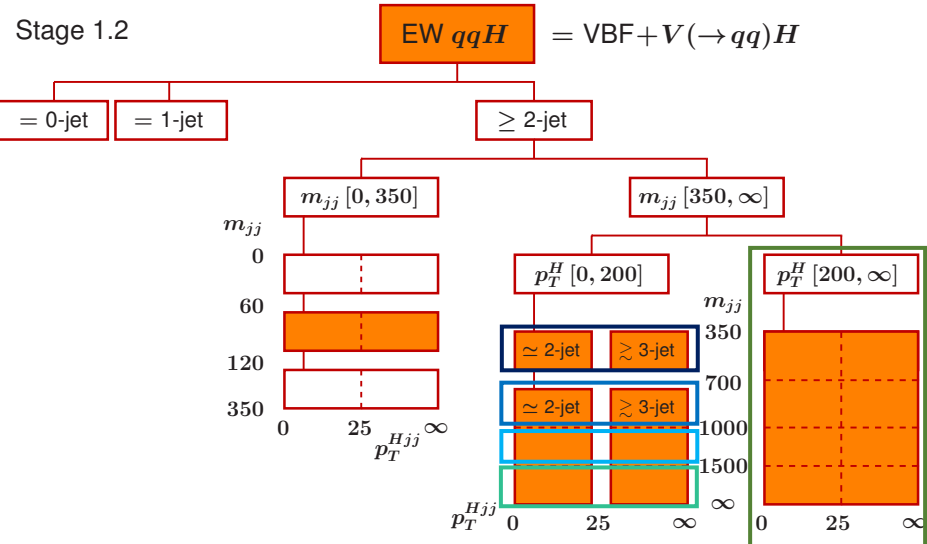
- ✓  $m_{ll} < 55 \text{ GeV}$
- ✓  $\Delta\phi_{ll} < 1.8$
- ✓  $|m_{jj} - 85| \leq 15 \text{ GeV}$  or  $\Delta y_{jj} > 1.2$
- ✓ Orthogonality with VBF analysis (fail central jet veto or outside lepton veto)

Control regions for top,  $qqWW$ ,  $Z/\gamma^*$  backgrounds.



Final discriminant:  $m_T$

# VBF $\geq 2$ -jet Signal Region



## Background rejection

- ✓  $N_{b-jet}^{p_T > 20 \text{ GeV}} = 0$
- ✓  $m_{\tau\tau} < m_Z - 25 \text{ GeV}$

## $H \rightarrow WW^* \rightarrow e\nu\mu\nu$ topology

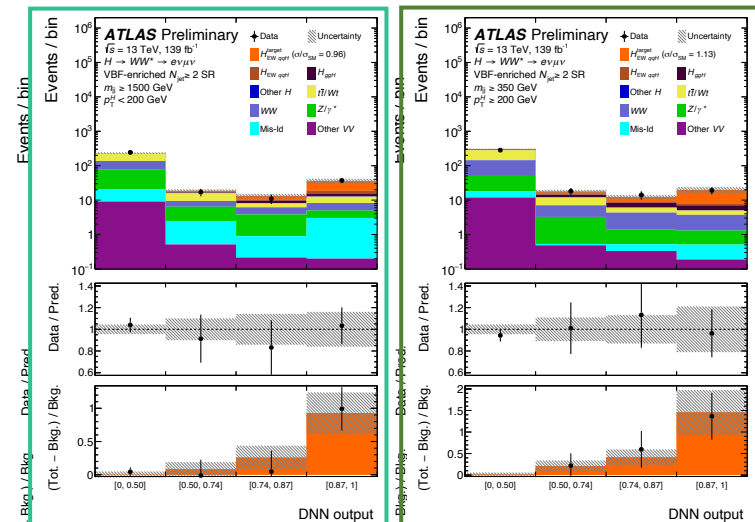
- ✓ Central jet veto ( $p_T > 30 \text{ GeV}$ )
- ✓ Outside lepton veto
- ✓  $m_{jj} > 120 \text{ GeV}$  (Orthogonality with VH analysis)

Control regions for top, Z/γ\* backgrounds.

Events sorted by Deep Neural Network (DNN) score based on 15 variables that target the VBF topology,  $H \rightarrow WW^*$  decay, and bkg (esp. top) suppression:

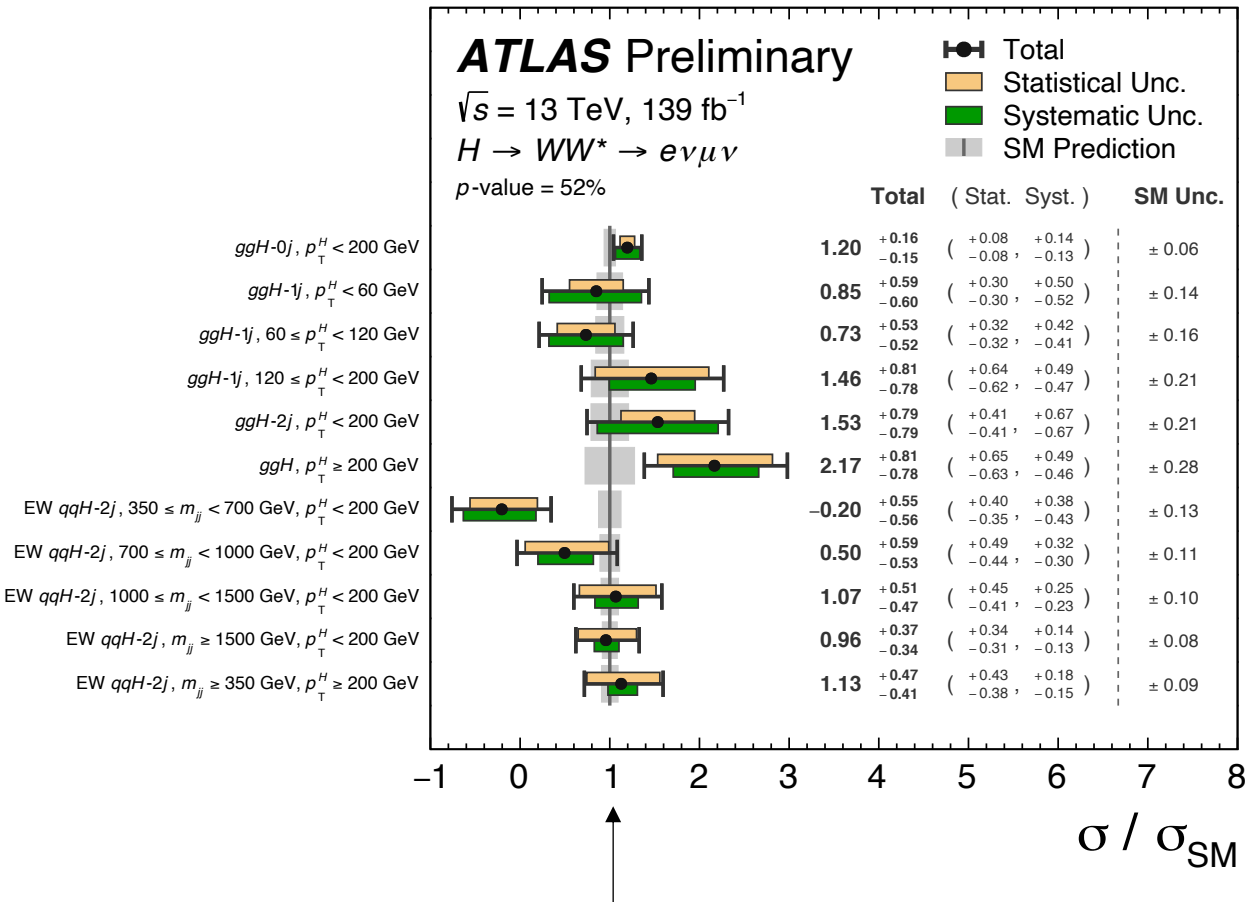
$\Delta y_{jj}, m_{jj}, \eta_\ell^{\text{centrality}}, m_{\ell 1 j 1}, m_{\ell 1 j 2}, m_{\ell 2 j 1}, m_{\ell 2 j 2}, p_T^{\text{jet}_1}, p_T^{\text{jet}_2}, p_T^{\text{jet}_3}, \Delta\phi_{\ell\ell}, m_{\ell\ell}, m_T, p_T^{\text{tot}}, \text{MET sig}$

Final discriminant: DNN output

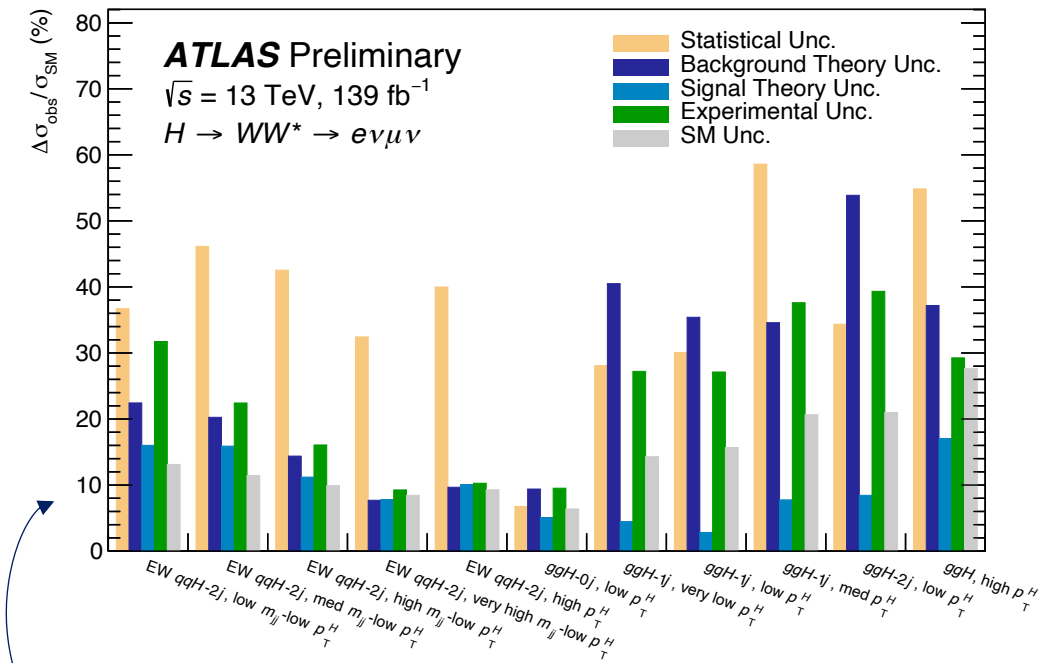


# Results

Ratio of measured cross-section to SM prediction shown for all 11 cross-sections:



Results are compatible with the SM.



Most analysis categories are **statistically-limited**, with some ggH modes affected predominantly by **background theory uncertainties**.

# Combined EFT Interpretation of $WW$ and $H \rightarrow WW^*$

---

Analysis Scope: [ATL-PHYS-PUB-2021-010](#)

- **Standard Model Effective Field Theory (SMEFT):** New physics enters at an energy scale  $\Lambda$ .
  - SM Lagrangian extended with higher-dimensional operators suppressed by powers of  $\Lambda$  and multiplied by Wilson coefficients  $c_i$ .
  - Measuring the coefficients probes BSM effects in a model-independent way.

$$\mathcal{L}_{\text{SMEFT}} = \mathcal{L}_{\text{SM}} + \sum_i \frac{c_i^{(5)}}{\Lambda} O_i^{(5)} + \sum_i \frac{c_i^{(6)}}{\Lambda^2} O_i^{(6)} + \dots$$

- This analysis uses the Warsaw basis.
- Simplified SMEFT formulation of the Lagrangian ignores odd-dimensional terms, truncates expansion at its leading order terms:

$$\mathcal{L}_{\text{SMEFT}} \approx \mathcal{L}_{\text{SM}}^{(4)} + \sum_i \frac{c_i^{(6)}}{\Lambda^2} O_i^{(6)} + \sum_j \frac{c_j^{(8)}}{\Lambda^4} O_j^{(8)}.$$

# Measurements Used

## Combining $WW$ and $H \rightarrow WW^*$

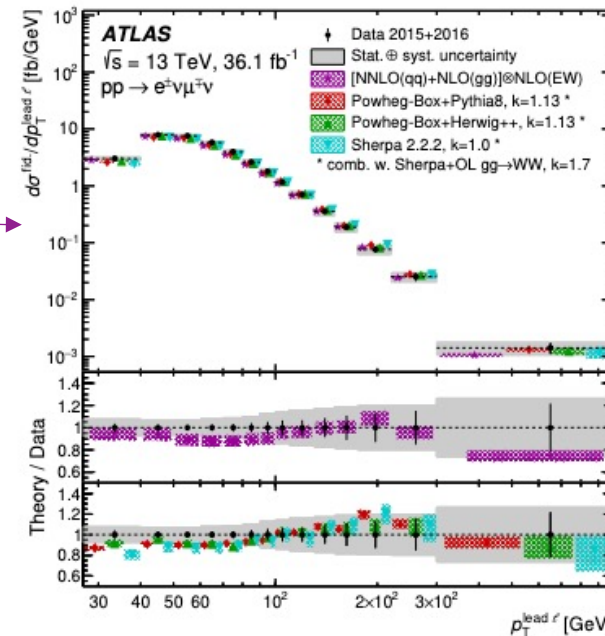
- This interpretation uses **two measurements**:

Partial Run 2 ( $36 \text{ fb}^{-1}$ ) equivalent of the  $H \rightarrow WW^* \rightarrow e\nu\mu\nu$  analysis described earlier in this talk, but only measuring total cross-sections (no STXS) [see [backup](#)].

- Total cross-sections of ggF and VBF Higgs production in the  $H \rightarrow WW^* \rightarrow e\nu\mu\nu$  channel at  $\sqrt{s}=13 \text{ TeV}$  [[arXiv: 1808.09054](#)]
- Fiducial and differential cross-sections of  $W^+W^-$  production at  $\sqrt{s}=13 \text{ TeV}$  [[arXiv: 1905.04242](#)]

Partial Run 2 ( $36 \text{ fb}^{-1}$ ). Use unfolded differential cross-section as a function of  $p_T^{\text{leading lepton}}$  due to its sensitivity to  $\mathcal{O}_i^6$  operators [see [backup](#)].

- Both sensitive to many SMEFT operators.
- Interpretation provides a case study in combining measurements to obtain constraints in the SMEFT framework.



# From Lagrangian to Cross-Section

---

Starting from the simplified SMEFT formulation of the Lagrangian:

$$\mathcal{L}_{\text{SMEFT}} \approx \mathcal{L}_{\text{SM}}^{(4)} + \sum_i \frac{c_i^{(6)}}{\Lambda^2} \mathcal{O}_i^{(6)} + \sum_j \frac{c_j^{(8)}}{\Lambda^4} \mathcal{O}_j^{(8)}.$$

Scattering cross-section becomes:

$$\sigma = |\mathcal{M}_{\text{SMEFT}}|^2 = \left| \mathcal{M}_{\text{SM}} + \sum_i \frac{c_i^{(6)}}{\Lambda^2} \mathcal{M}_i^{(6)} \right|^2 + \mathcal{O}(\Lambda^{-4}) = |\mathcal{M}_{\text{SM}}|^2 + \underbrace{\sum_i \frac{c_i^{(6)}}{\Lambda^2} 2\text{Re} \left( \mathcal{M}_i^{(6)} \mathcal{M}_{\text{SM}}^* \right)}_{\text{SM matrix element}} + \underbrace{\mathcal{O}(\Lambda^{-4})}_{\substack{\text{Contains } \mathcal{O}_i^6 \\ \text{Contains } \mathcal{O}_i^8; \\ \text{neglected}}}.$$

Linearized cross-section times branching ratio for a process  $p$ :

$$\sigma^p \mathcal{B}^{H \rightarrow e\mu\nu\nu} = \underbrace{\sigma_{\text{SM}}^p \mathcal{B}_{\text{SM}}^{H \rightarrow e\mu\nu\nu}}_{\text{SM cross-section times BR}} \left( 1 + \sum_i A_i^p c_i + \sum_i c_i B_i^{H \rightarrow e\nu\mu\nu} - \sum_i c_i B_i^{\text{tot}} \right) + \mathcal{O}(\Lambda^{-4}).$$

Linear effect of the operator associated with  $c_i$  on  $\sigma$  or the partial or total Higgs width.

Contains  $\mathcal{O}_i^8$ ; neglected

# Ingredients for a Combined EFT Interpretation

---

- **Operators:** 24 Warsaw basis operators affect the signal processes ( $WW$  production, and  $ggF$  and  $VBF$  Higgs production)
  - ✓ All CP-even; CP-odd operators have no effect in the linearized approximation.
- **Orthogonal SRs and CRs:** The  $HWW$  0-jet and 1-jet  $WW$  CRs overlap with the  $WW$  SR.
  - ✓ Remove the  $HWW$   $WW$  CRs from the fit; use the  $WW$  SR to constrain the  $WW$  background in  $HWW$  instead.
- **Acceptance corrections:** The  $HWW$  measurement includes acceptance effects (not fiducial).
  - ✓ Calculate acceptance effects for each SMEFT interference sample.
  - ✓ Correct via linear coefficients of operators that have acceptance effects.
- **Combined likelihood:**
  - ✓ Likelihood functions for  $HWW$  and  $WW$  re-parameterized as functions of the Wilson coefficients.

$$L^{\text{comb}}(N, \mathbf{x} | \mathbf{c}, \boldsymbol{\theta}^{\text{comb}}) = \prod_{b \notin \text{WW-CR}}^{n_{\text{bins}}^{\text{SR+CR}}} \text{Poisson}\left(N_b \left| \sum_p \mu_p(\mathbf{c}) S_p(\boldsymbol{\theta}^{HWW}) + B(\mathbf{c}, \boldsymbol{\theta}^{HWW})\right.\right)$$
$$\times \frac{1}{\sqrt{(2\pi)^{n_{\text{bins}}^{\text{WW}}} \det(C)}} \exp\left(-\frac{1}{2} \Delta \mathbf{x}(\mathbf{c}, \boldsymbol{\theta}^{WW})^\top C^{-1} \Delta \mathbf{x}(\mathbf{c}, \boldsymbol{\theta}^{WW})\right) \times \prod_i^{n_{\text{syst}}^{\text{comb}}} f_i(\theta_i^{\text{comb}}).$$

Likelihood for observing  $N$  events  
in the  $H \rightarrow WW^*$  analysis bins,  
and measuring differential cross-  
section of  $\mathbf{x}$  in the  $WW$  analysis.

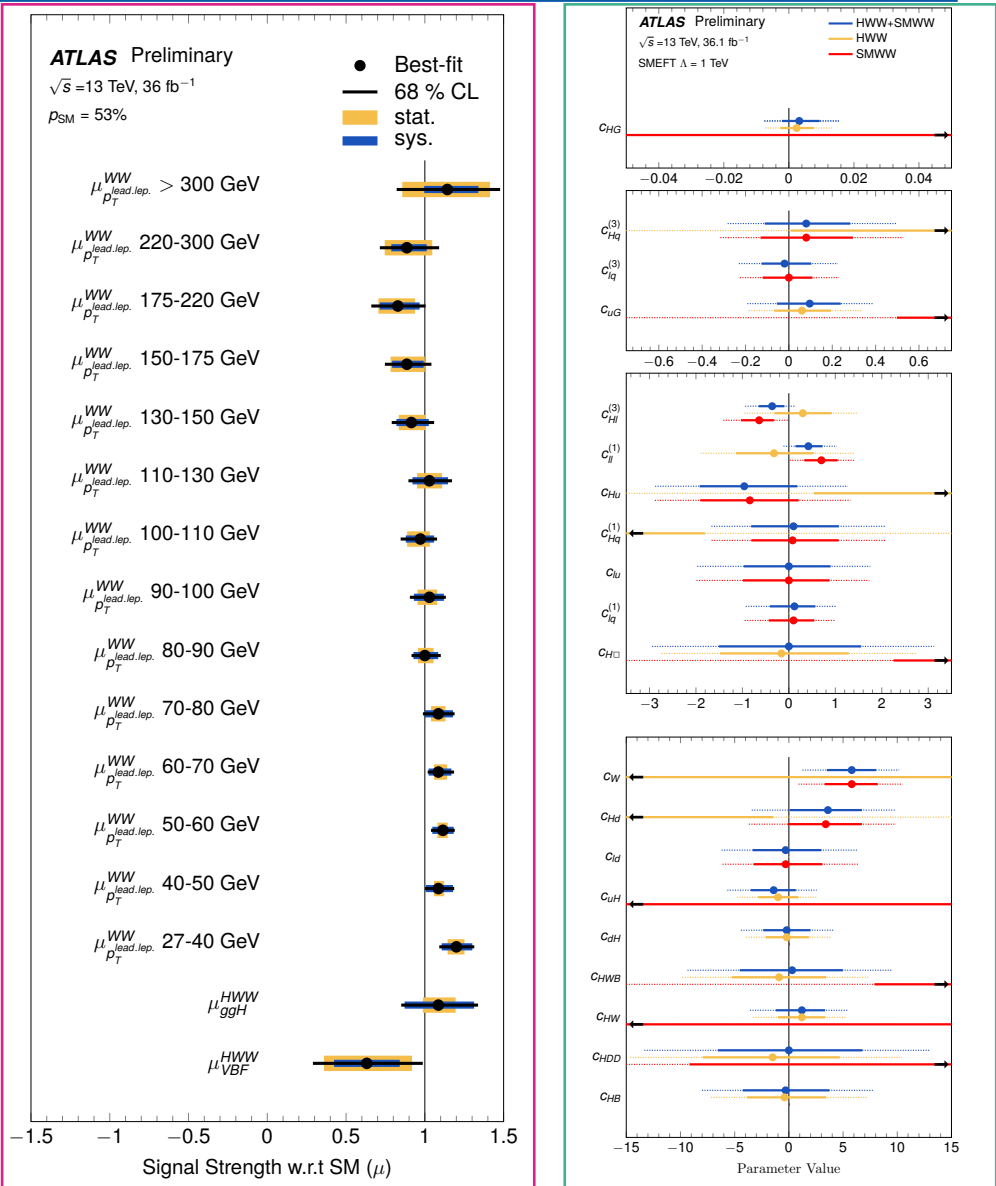
# Results (1)

## Signal strength measurements

- Simultaneously measure  $\mu_{ggF}$ ,  $\mu_{VBF}$ , and 14  $\mu$  values for  $WW$  leading lepton  $p_T$  bins.
- Results are compatible with standalone analyses.
- Non-identical results come from removal of the  $WW$  CR from ggF HWW, and pulls on correlated nuisance parameters in the new fit.

## Individual Wilson coefficient limits

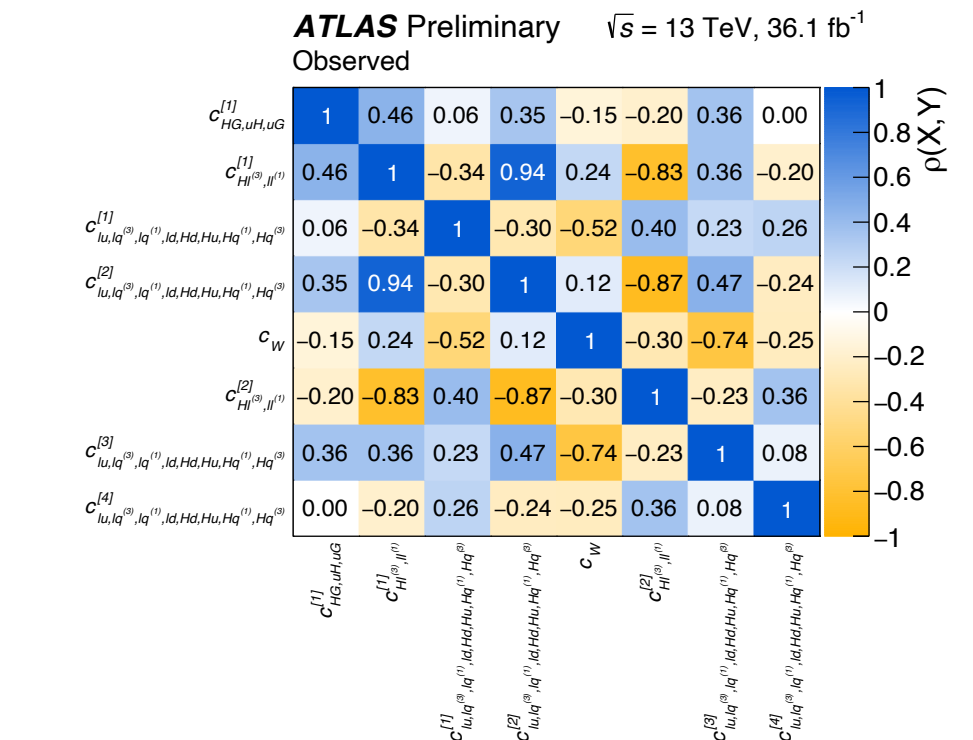
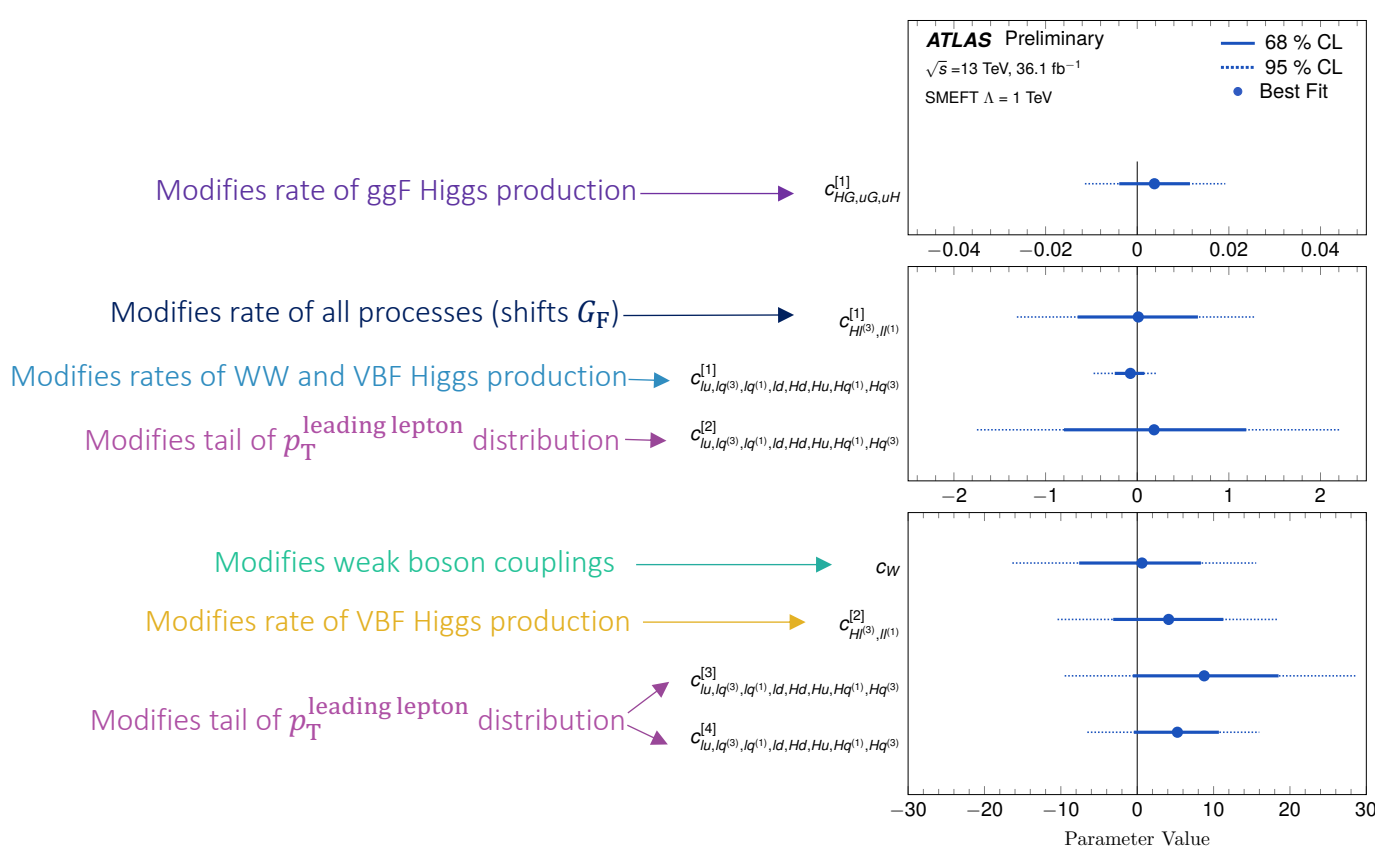
- Fit for each coefficient, with all others **fixed to SM value of 0**.
- Resulting constraints agree with SM within  $2\sigma$  or better.
- See sensitivity gain from combining for most operators.



# Results (2)

## Simultaneous Wilson coefficient limits

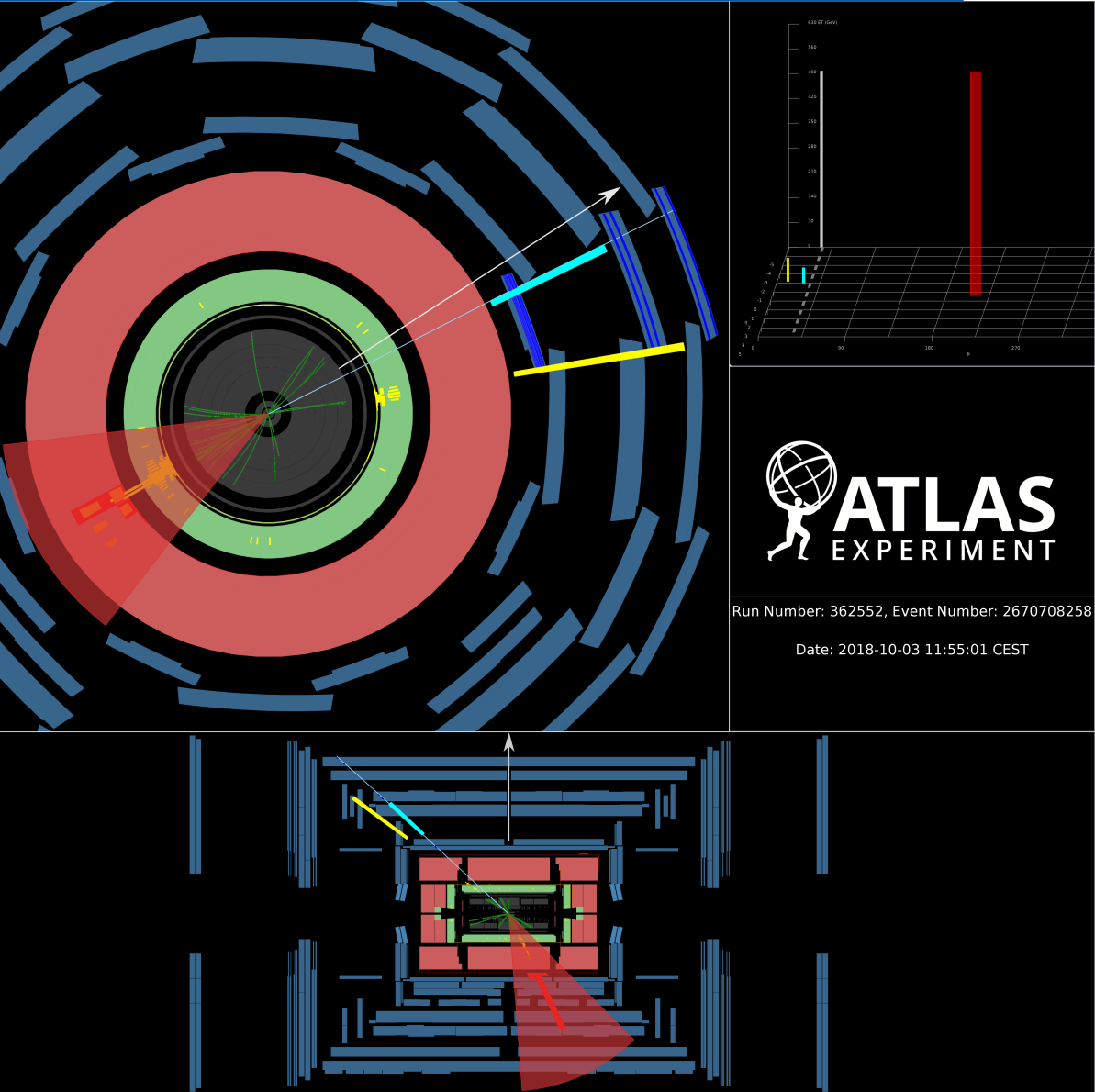
- Not enough information to constrain all coefficients in a maximum likelihood fit.
  - Determine modified basis of Warsaw vectors following [ATL-PHYS-PUB-2019-042, ATLAS-CONF-2020-053]
- Results in 8 physically-interpretable parameter groupings.



✓ **Conclusions:** Parameters are consistent with the SM, and four parameters are determined with a precision  $< 1$ .

# Conclusions

- Measurements of STXS and fiducial (differential) cross-sections have many advantages, including allowing for combination and interpretation in an EFT framework.
- $H \rightarrow WW^*$  offers a well-understood, sensitive channel that lends itself to further precision tests of the SM.
- Completing the landscape of ATLAS  $H \rightarrow WW^*$  cross-sections and interpretations:
  - [arXiv:1903.10052](#): Measurement of total  $ZH$  and  $WH$  cross-sections with  $36\text{ fb}^{-1}$  of Run 2 data [see [backup](#)].
  - [arXiv:2109.13808](#): Measurement of CP properties of the effective Higgs-gluon vertex, and polarization-dependent Higgs coupling strengths to W and Z bosons [see [Chiara Arcangeletti's talk](#)].
- The recent results presented here show how  $H \rightarrow WW^*$  decays can be exploited for sensitive measurements and interpretations of Higgs boson physics.



# Backup

# $VH H \rightarrow WW^* (1)$

Analysis Scope: [arXiv:1903.10052](https://arxiv.org/abs/1903.10052)

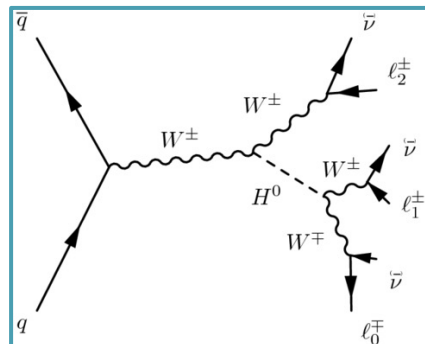
- $WH$  and  $ZH$  production of Higgs bosons in the  $H \rightarrow WW^* \rightarrow l\nu l\nu$  decay channel.
- Uses  $36 \text{ fb}^{-1}$  of Run 2 data.

## Analysis Strategy

- Channels defined by number of final-state leptons:  $3l$  channel targets  $WH$ ,  $4l$  channel targets  $ZH$ .
- Events further split into categories according to the number of same-flavour, opposite-sign (SFOS) pairs:

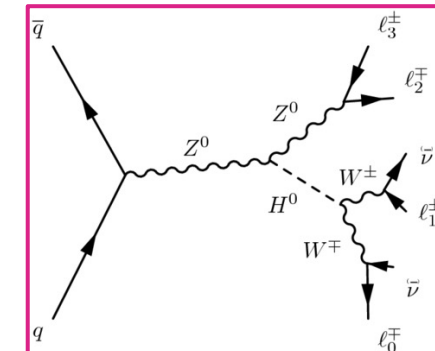
$WH$ :

- Events with 1 SFOS pair = “Z-dominated”
- Events with 0 SFOS pairs = “Z-depleted”



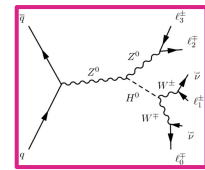
$ZH$ :

- Events with 2 SFOS pairs
- Events with 1 SFOS pairs



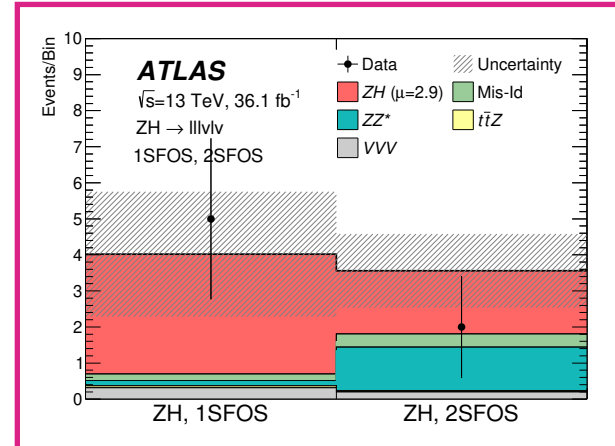
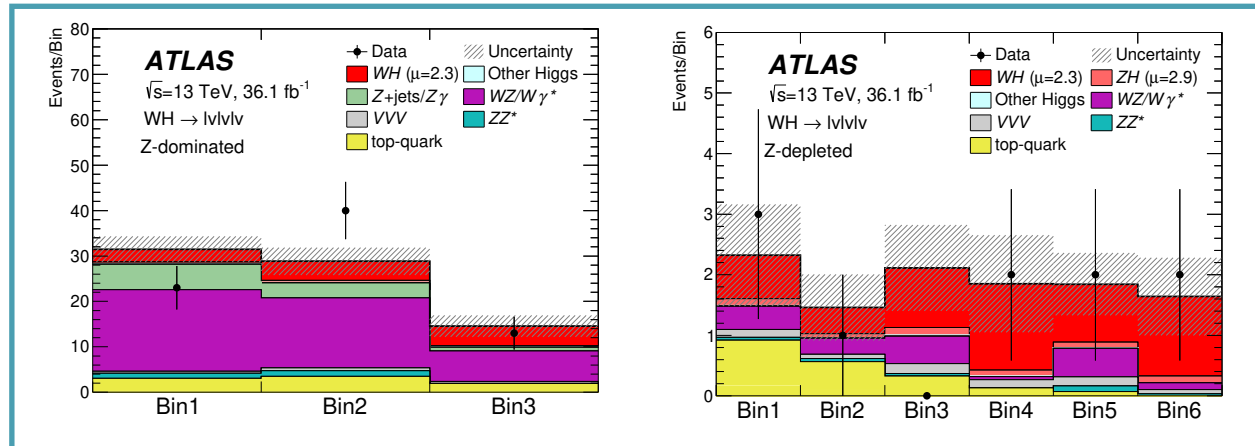
Number of SFOS pairs has a large effect on background composition

# $VH H \rightarrow WW^*$ (2)



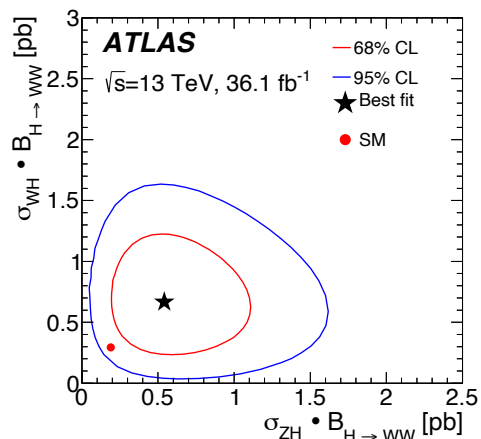
## Results

- Profile likelihood fit uses binned distributions of **WH BDTs**, event counts in CRs, and event counts in **ZH SRs**.



$$\begin{aligned}\sigma_{WH} \cdot \mathcal{B}_{H \rightarrow WW^*} &= 0.67^{+0.31}_{-0.27}(\text{stat.})^{+0.14}_{-0.11}(\text{exp syst.})^{+0.11}_{-0.09}(\text{theo syst.}) \text{ pb}, \\ \sigma_{ZH} \cdot \mathcal{B}_{H \rightarrow WW^*} &= 0.54^{+0.31}_{-0.24}(\text{stat.})^{+0.10}_{-0.05}(\text{exp syst.})^{+0.11}_{-0.05}(\text{theo syst.}) \text{ pb}.\end{aligned}$$

1D fit results are consistent with the SM within  $1.3\sigma$  for  $WH$  and  $1.5\sigma$  for  $ZH$ .



# ggF and VBF $H \rightarrow WW^*$ 36 fb $^{-1}$ Measurement

Analysis Scope: [arXiv: 1808.09054](https://arxiv.org/abs/1808.09054)

- Measurement of ggF and VBF cross-sections and signal strengths in the  $H \rightarrow WW^*$  channel using partial Run 2 data.

## Analysis Strategy

- Very similar to full Run 2 analysis described in this talk, with a few differences:
  - No ggF 2-jet channel.
  - BDT as final VBF discriminant.
  - Does not target STXS bins.

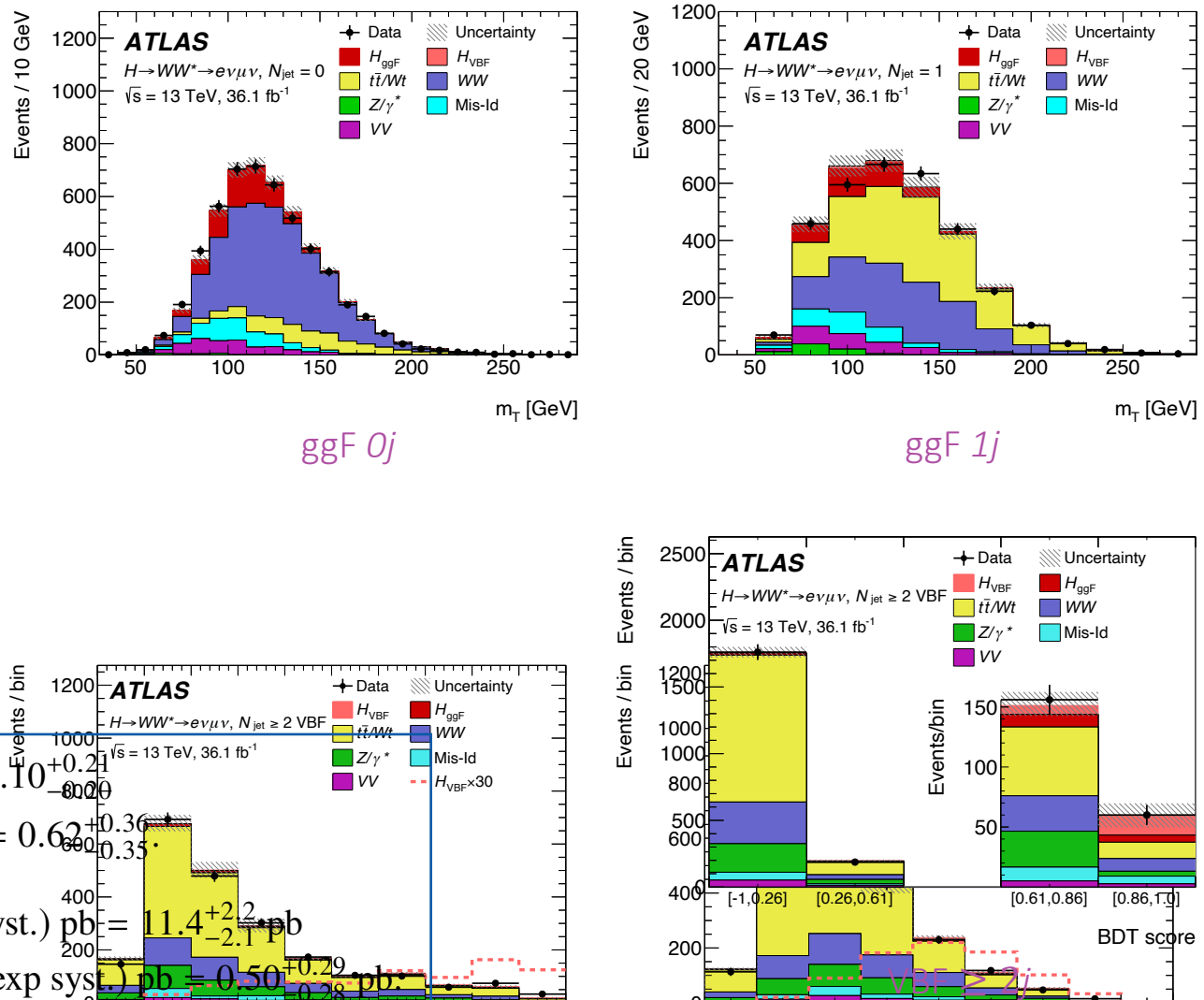
## Results

$$\mu_{\text{ggF}} = 1.10^{+0.10}_{-0.09}(\text{stat.})^{+0.13}_{-0.11}(\text{theo syst.})^{+0.14}_{-0.13}(\text{exp syst.}) = 1.10^{+0.21}_{-0.20}$$

$$\mu_{\text{VBF}} = 0.62^{+0.29}_{-0.27}(\text{stat.})^{+0.12}_{-0.13}(\text{theo syst.}) \pm 0.15(\text{exp syst.}) = 0.62^{+0.36}_{-0.35}.$$

$$\sigma_{\text{ggF}} \cdot \mathcal{B}_{H \rightarrow WW^*} = 11.4^{+1.2}_{-1.1}(\text{stat.})^{+1.2}_{-1.1}(\text{theo syst.})^{+1.4}_{-1.3}(\text{exp syst.}) \text{ pb} = 11.4^{+2.2}_{-2.1} \text{ pb}$$

$$\sigma_{\text{VBF}} \cdot \mathcal{B}_{H \rightarrow WW^*} = 0.50^{+0.24}_{-0.22}(\text{stat.}) \pm 0.10(\text{theo syst.})^{+0.12}_{-0.13}(\text{exp syst.}) \text{ pb} = 0.50^{+0.29}_{-0.28} \text{ pb}.$$



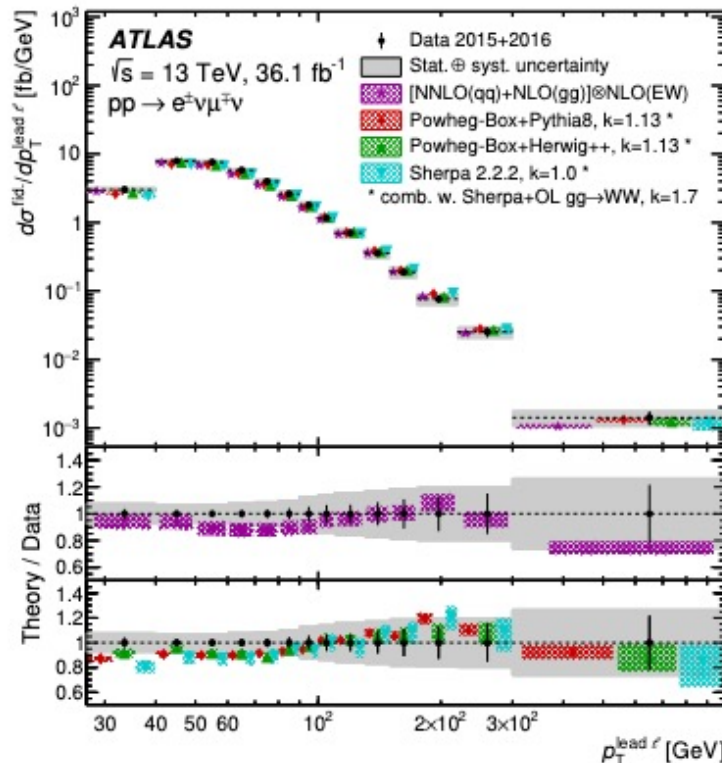
# $WW$ $36 \text{ fb}^{-1}$ Differential and Fiducial Measurement

Analysis Scope: [arXiv: 1905.04242](https://arxiv.org/abs/1905.04242)

- Measurement of differential and fiducial cross-sections in the  $WW \rightarrow e\nu\mu\nu$  channel using partial Run 2 data.

## Results

- Fiducial cross-section measured in total, and in bins of various observables (leading lepton ( $p_T^{\text{lead}}$ ) used for EFT interpretation).



## Analysis Strategy

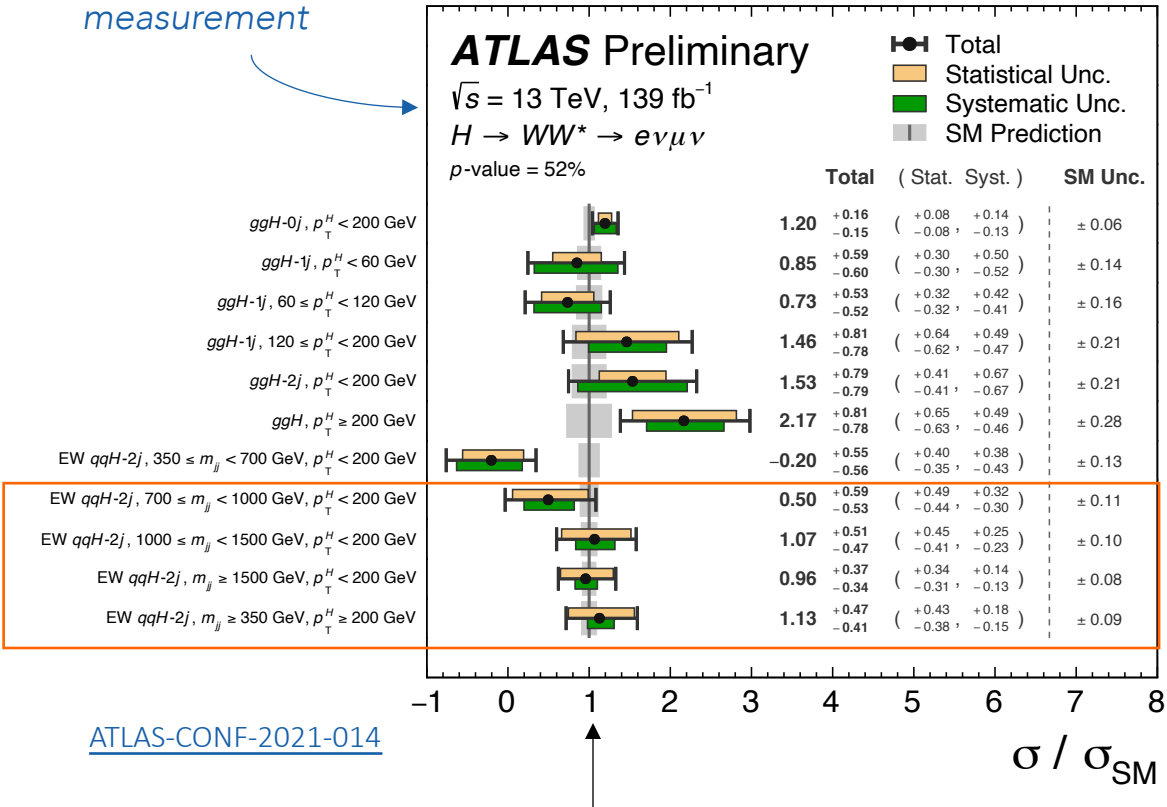
- $WW$  candidate event selection: Similar to  $H \rightarrow WW^*$  0j SR but with inverted  $m_{e\mu}$  cut.

Selection requirement	Selection value
$p_T^\ell$	$> 27 \text{ GeV}$
$\eta^\ell$	$ \eta^e  < 2.47$ (excluding $1.37 <  \eta^e  < 1.52$ ), $ \eta^\mu  < 2.5$
Lepton identification	<i>TightLH</i> (electron), <i>Medium</i> (muon)
Lepton isolation	<i>Gradient</i> working point
Number of additional leptons ( $p_T > 10 \text{ GeV}$ )	0
Number of jets ( $p_T > 35 \text{ GeV}$ , $ \eta  < 4.5$ )	0
Number of $b$ -tagged jets ( $p_T > 20 \text{ GeV}$ , $ \eta  < 2.5$ )	0
$E_{\text{T}}^{\text{miss,track}}$	$> 20 \text{ GeV}$
$p_T^{e\mu}$	$> 30 \text{ GeV}$
$m_{e\mu}$	$> 55 \text{ GeV}$

- Main bkg from top: estimated using partially data-driven method (extrap. from top CR to SR).
  - Mis-identified lepton bkg also from data-driven method; rest from MC.
- $b$ -tagging uncertainty dominates.

# ggF and VBF $H \rightarrow WW^*$ STXS Measurement

$H \rightarrow WW^*$   
standalone  
measurement



Results are compatible with the SM and (for VBF)  
competitive with the Summer 2020 combination of  
all Higgs results measured with the ATLAS detector.

